Catalyst Evolution in Ruthenium-Catalyzed Coupling of Amines and Alcohols

Valeriy Cherepakhin and Travis J. Williams*

Donald P. and Katherine B. Loker Hydrocarbon Institute and Department of Chemistry, University of Southern California, Los Angeles, California, 90089-1661, United States.

ABSTRACT: We describe the mechanism, scope, and catalyst evolution for our ruthenium-based coupling of amines and alcohols, which proceeds from a $[(\eta^6\text{-cymene})\text{RuCl}(\text{PyCH}_2\text{PBu}_2^t)]\text{OTf}(\mathbf{1})$ precatalyst. The method selectively produces secondary amines through a hydrogen borrowing mechanism and is successfully applied to several heterocyclic carbinol substrates. Under the reaction conditions, precatalyst **1** evolves through a series of catalytic intermediates: $[(\eta^6\text{-cymene})\text{RuH}(\text{PyCH}_2\text{PBu}_2^t)]\text{OTf}(\mathbf{3})$, $[\text{Ru}_3\text{H}_2\text{Cl}_2(\text{CO})(\text{PyCH}_2\text{PBu}_2^t)_2\{\mu\text{-}(C_5\text{H}_3\text{N})\text{CH}_2\text{PBu}_2^t\}]\text{OTf}(\mathbf{4})$, and a diastereomeric pair of $[\text{Ru}_2\text{HCl}(\text{CO})_2(\text{PyCH}_2\text{PBu}_2^t)_2(\mu\text{-O}_2\text{CPr}^n)]\text{X}$ (trans-**5**, X = Cl; cis-**6**, X = OTf). The structures of **4** and **6** were established by single-crystal X-ray diffraction. A study of catalytic activity shows that **4** is a dormant (but alive) form of the catalyst, whereas **5** and **6** are the ultimate dead forms. Electrochemical studies show that **4** is redox-active and undergoes electrochemically-reversible one-electron oxidation at $E_{1/2}$ = 0.442 V (vs. Fc⁺/Fc) in CH₂Cl₂ solution. We discuss the factors that govern formation of **3** – **6** and the role of selective ruthenium carbonylation, which is essential for enabling generation of the active catalyst. We also connect these discoveries to the identification of conditions for amination of aliphatic alcohols, which eluded us until we understood the catalyst's complex speciation behavior.

KEYWORDS Alcohol, Amine, Hydrogen Borrowing, Ruthenium, Metal Hydride, Metal Cluster

INTRODUCTION

Over the last decade many ruthenium-based catalytic systems have been developed that enable alcohol-amine coupling through hydrogen borrowing. This reaction is of vital importance because of its relevance to the efficient preparation of medicinal synthons. We divide the known catalysts into three structural groups. First, some catalysts are formed in situ from a metal precursor (such as Ru₃(CO)₁₂₁¹⁻⁵ $[RuCl_2(\eta^6-p\text{-cymene})]_{2}^{6-13}$ $[RuCl_2(COD)]_{n}$, 14 RuCl₂(PPh₃)₃,⁷ [Cp*RuCl₂]₂₁¹⁵ or RuCl₃·xH₂O¹⁶) and a phosphine. Second, some proceed from arene complexes, e.g. $[(\eta^6\text{-arene})\text{RuClL}_2]X^{17-21}$ or $[(\eta^6\text{-arene})\text{RuClL}_2]X^{17-21}$ arene) $RuCl_2L$]^{18,22} (L = PR₃, NHC, Py, SR₂, SeR₂; X = Cl, PF₆, OTf). Third, there are several excellent pincer complexes of PNN,23 PNO/ PNS,²⁴ PNP,²⁵ and NNC²⁶ types (Figure 1) that typically contain RuH(CO) fragments and operate through a metal-ligand cooperative mechanism that is enabled by deprotonation of CH₂PR₂ group. About half of the reported methods proceed from arene complexes (the second group), but very little is known about the bonding and speciation of ruthenium in these catalyst systems. Although some authors sketch intermediates and catalytic cycles for their systems, 10,15,18,19,22,24 we find most these proposals not to be supported by experiment, and we see that few address precatalyst speciation and activation, which are almost certainly not simple when an (arene)ruthenium complex is introduced into a solution of amines and alkoxides.

Understanding composition, structure, and reactivity of catalytic intermediates is crucial for systematic comprehension and analysis of reaction mechanisms and the ways in which different ligands govern catalytic activity, turnover, and deactivation of a homogeneous catalyst: it's impossible to tell a story until you know the characters. While such understanding ultimately can direct design of new, more prolific catalytic systems, we see little detailed work on this problem for these arene-ligated ruthenium-based amination catalysts. Moreover, we have

characterized unexpected transformations of precatalytic species including ligand derivatization and displacement, ligation with substrate degradation products, cluster formation, etc. with a number of ruthenium- and iridium-based precursors that we expected to behave simply.²⁷

We recently reported a ruthenium complex $[(\eta^6 - cymene)RuCl(PyCH_2PBu^1_2)]OTf$ (1, Figure 1) that efficiently catalyzes coupling of primary amines and benzylic alcohols without the aid of a strong base. In this study we extend the reaction scope to aliphatic alcohols and certain heterocyclic carbinols. Our identification of these conditions presaged a complicated story of why we had not found them before. To answer this, we present a study on the speciation and life cycle of the ruthenium complexes in this reaction and show how the story reveals the way that precatalyst 1 activates, reacts, deactivates, and dies.

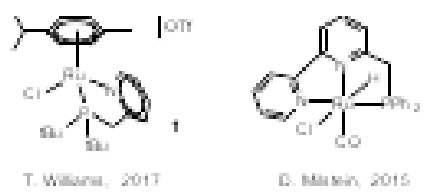


Figure 1. Precatalysts for Alcohol-Amine Coupling.

RESULTS AND DISCUSSION

Coupling of Aliphatic Amines and Alcohols

We developed complex 1 as a catalyst for *N*-alkylation of primary amines with benzylic alcohols, which left an opportunity to optimize the system for aliphatic alcohols. We found excellent results with catalyst loadings down to 1 mol% in our original study. While benzyl alcohols react smoothly with this catalyst loading, providing secondary

amines with excellent yield and selectivity, aliphatic alcohols, tended to overalkylate and proceed in low efficiency, giving an undesirable yield and selectivity of amine products. Here we demonstrate *cutting the catalyst load even further* slows down the overalkylation by aliphatic alcohol and enables selective, high yielding formation of secondary amine products that we were not able to achieve with our initial conditions.

We demonstrate this finding by using 1-aminohexane and 1-butanol as representative substrates at 0.2 mol% Ru loading (Table 1). In the absence of alcohol (entry 1) 1-aminohexane undergoes slow homocoupling to give dihexylamine and NH3. When 1-butanol is present, the homocoupling route is halted and amine-alcohol coupling becomes the major reaction pathway (entries 2-4). The catalytic system exhibits high selectivity of amine monoalkylation by providing 98% yield of N-butylhexylamine (entry 2). Increasing the alcohol/amine ratio above 1:1 does not significantly affect the product distribution indicating slowness of the second alkylation step. Thus, the catalytic system is highly selective for secondary amine formation. Possible byproducts, such as amides, esters, carboxylates, and imines are not detected. Imine formation is easily suppressed by conducting the reaction in a closed reactor. Although the reaction is rapid (full conversion is reached within 1 hour with 1.0 mol% Ru), we find that the catalyst fails to give full conversion of 1-aminohexane at loadings below 0.05 mol% (vide infra).

Table 1. Coupling of 1-Aminohexane with 1-Butanol.^a

[BuOH]/	HexNH ₂ ,	Hex ₂ NH,	HexNHBu,	HexNBu ₂ ,
[HexNH ₂]	%b	%	%	%
0	62	38	-	-
1	0	0	98	2
2	0	0	93	7
3	0	0	93	7
	[BuOH]/ [HexNH ₂] 0 1 2 3			0 62 38 - 1 0 0 98 2 0 0 93

 a Reaction conditions: a mixture of 1-aminohexane (100 mg, 9.88 x 10 4 mol), 1-butanol, and complex 1 (1.3 mg, 2.0 μmol) was stirred in a closed reactor at 110 o C for 36 h. b The yields were calculated from 1 H NMR spectra.

We compared catalytic activity of complex 1 and the known alcoholamine coupling catalysts, such as $[(\text{cymene})\text{RuCl}_2]_2\text{-dppf},^{10,12,13}$ Shvo complex, 28 Ru $_3$ (CO) $_{12}$ –PPh $_3$, 1,2,4,5,29 CpRuCl(PPh $_3$) $_2$ 30 and RuH $_2$ (CO) (PPh $_3$) $_3$ (Table S1). Complexes 1 and CpRuCl(PPh $_3$) $_2$ enable conversion of 1-aminohexane at 100% and 15%, respectively, while others show no catalytic activity ([BuOH]/[HexNH $_2$] = 1.5, 1.0 mol% Ru, 110 °C, 1 h). Thus, 1 exhibits superior catalytic activity among the tested complexes under the specified conditions.

The scope of alcohol-amine coupling with precatalyst 1 can be successfully extended to heterocyclic substrates, such as pyridines, thiophenes, and indoles (Table 2). Acidic substrates, such as phenols (entry 2), can be reacted since the system does not need a strong base to activate the catalyst.

Table 2. Expansion of Substrate Scope for Amine-Alcohol Coupling.^a

$$R_1$$
 NH_2 + R_2 OH $Complex 1$ R_1 N R_2 + H_2O

En- try	Alcohol Amine	Product	Catalyst, % Time, h Yield, %
1 ^b	NH ₂	NH A	0.2 36 90
2	HO BuOH	NHBu B	0.4 42 70
3	Me O BuOH	√le O NHBu	0.4 30 83
4	BuOH NH ₂	D NHBu	0.4 30 81
5°	S OH	S E NHHex	0.7 42 62
6 ^b	NH ₂ N BuOH	NHBu NHBu	0.2 20 74

^a Reaction conditions: a mixture of amine (2.0 mmol), alcohol (3.0 mmol), and complex **1** was stirred for required period in a closed reactor at 110 °C. ^b Alcohol loading is 2.0 mmol. ^c Alcohol loading is 1.3 mmol.

Time-Course Study; Synthesis and Characterization of Ruthenium Complexes

Discovery of improved catalyst performance at reduced catalyst loadings presaged a very interesting story about dimerization, cluster formation, or some combination of multi-metallic pathways that could be involved in the process, probably to the detriment of catalyst turnover. Despite its potential complexity, we determined to uncover this story.

We started looking into catalyst speciation with a time-course study using a stoichiometric loading of precatalyst ${\bf 1}$ with 1-butanol and 1-aminohexane as coupling partners. These starting materials are particularly convenient for this purpose, since they allow a reaction at high temperature and are easily separated from reaction mixture. This facilitates analysis and isolation of ruthenium intermediates. In a typical experiment the molar ratio of $[{\bf 1}]$:[HexNH $_2$]:[BuOH] was 1:6.5:144. The reaction was performed in a closed reactor at 110 °C, then the organic materials were removed under vacuum and the residue was analyzed by 1 H and 3 1P NMR spectroscopy (Figure S22).

Initially, the reaction was terminated after three minutes. According to ^{31}P NMR, two major ruthenium species in ca. 1 : 1 ratio are present in the system at this point: complex 1 (^{31}P $\delta=87.31$ ppm) and a new ruthenium compound (3) that gives a doublet at ^{31}P $\delta=109.75$ ppm ($^{2}J_{PH}=42.8$ Hz). The ^{1}H NMR spectrum contains the corresponding doublet at -8.65 ppm, which is characteristic of a metal hydride ligand. Thus, complex 3 is a product of chloride replacement by hydride to give [(η^{6} -cymene)RuH(PyCH₂PBut₂)]OTf. Fractional crystallization failed to separate 3 from 1, therefore, we confirmed its identity by independent synthesis from 1.

Scheme 1. Synthesis of Intermediate 3.

 $[RuCl_2(\eta^6\text{-cymene})],$ converts $[(\eta^6$ cymene)RuH(PPh₃)₂]+ when treated with AgPF₆ and PPh₃ in methanol at 25 °C,31 treatment of 1 with AgOTf in the presence of alcohols gives high yield of the corresponding triflate complex, $[(\eta^6$ cymene)Ru(OTf)(PyCH₂PBu^t₂)]OTf (2), rather than the hydride (Scheme 1). The ¹⁹F NMR spectrum of 2 in CD₂Cl₂ solution contains two distinct peaks at -78.66 and -78.82 ppm with equal intensities, belonging to the coordinated and free triflate groups. Complex 2 reacts reversibly with 2-propanol to give hydride 3 (Scheme 1). Its formation is favored at 110 °C in a closed reactor; rapid removal of acetone under vacuum provided the product in 50% yield. At room temperature the equilibrium is completely shifted to the right. We showed this by reacting 3 with HOTf in acetone- d_6 to give rapid and selective formation of 2 as identified by its ³¹P peak at 91.03 ppm. The chemical shifts of the phosphine (31 P δ = 109.75 ppm) and hydride (1 H δ = – 8.65 ppm) ligands are identical for the compound obtained in this reaction and for the compound detected in the catalytic reaction after three minutes. Thus, complex 3 is the first ruthenium intermediate in the sequence of precatalyst speciation.

As the reaction proceeds among complex 1, 1-aminohexane, and 1butanol, the color of the reaction solution changes from orange-red to black-green within 30 minutes. If the reaction is stopped after 1 hour, a black crystalline compound, 4, is isolated with 63% yield (Scheme 2). The structure of 4 was established by single-crystal X-ray diffraction (Figure 2). The complex is a trinuclear cluster formed by three Ru(II) atoms and arranged in an asymmetrical triangular fashion. The observed Ru-Ru distances (2.717, 2.897, and 2.907 Å) are near Ru-Ru distances in Ru₃(CO)₁₂³² Ru₃Cl₆(PCy₃)₃³³ and ruthenium metal³⁴ (2.854, 2.593, and 2.649 Å, respectively), indicating significant intermetallic interaction within Ru₃ core. We omit these bonds from the structural diagram for clarity's sake only. Complex 4 features orthometalated bridging pyridyl ligand coordinated to Ru-CO group. This carbonyl ligand appears to derive from our starting alcohol, by analogy to an iridium-based alcohol oxidation system that we have recently characterized.²⁷ While the ortho-metalated pyridyl fragment is a common substructure in ruthenium carbonyl clusters,35-37 typically derived from Ru₃(CO)₁₂ complex 4 is a unique example of tandem selective monocarbonylation, pyridine ortho-metalation, and cluster self-assembly all happening from a mononuclear precursor.

Scheme 2. Synthesis of Intermediate 4.

Complex 4 was characterized by multinuclear NMR spectroscopy in CD₂Cl₂ solution. In its 1H spectrum, 4 presents two hydride ligands with chemical shifts at -16.50 (ddd, $^2J_{PH}=51.6,\,27.3,\,9.1$ Hz) and -21.36 (dd, $^2J_{PH}=20.0,\,4.5$ Hz) ppm. These hydrides do not correlate in a COSY spectrum, meaning that their peak multiplicities originate from $^1H-^{31}P$ coupling. We use this feature to justify location and coordination mode of the hydrides. Based on coupling pattern of the peaks at -16.50 and -21.36 ppm we attribute them to $\mu_3\text{-H}$ and $\mu\text{-H}$ ligands, respectively. This assignment fulfils coordinative saturation of all ruthenium atoms in the molecule. ^{31}P NMR data are consistent with three inequivalent PN ligands (^{31}P $\delta=128.34,\,116.38,\,$ and 89.76 ppm).

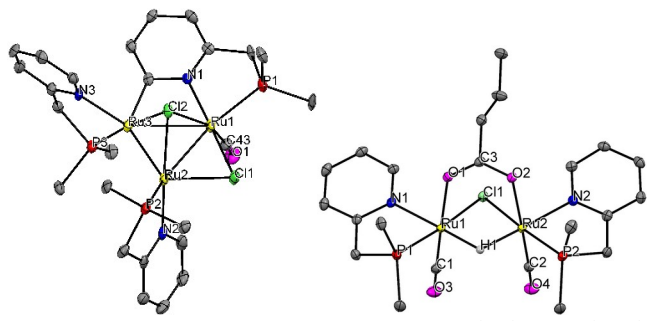
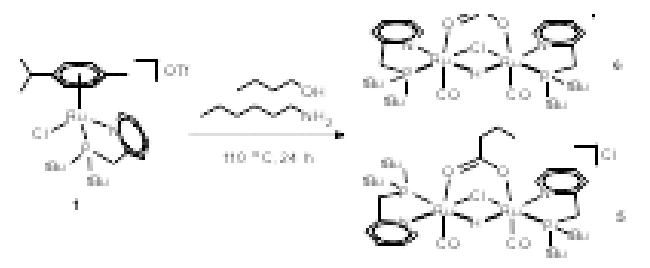


Figure 2. Molecular structures of the cations of **4** (left) and **6** (right) shown with 50% probability ellipsoids. Hydrogen atoms and methyl groups are omitted for clarity.

Complex 1 is further derivatized when treated with an excess of 1-aminohexane (> 10 equivalents, Scheme 3). After 24 hours, two major complexes, 5 and 6, were detected by their hydride peaks at 1H $\delta = -15.34$ and -21.03 ppm, respectively. Complexes 5 and 6 are formed in ca. 1:1 ratio, and they persist even when 100 equivalents of 1-aminohexane is used (Figure S24). Chromatographic purification followed by crystallization afforded 6-CH $_2$ Cl $_2$ in 18% yield. Although we failed to obtain a pure sample of 5 from this reaction mixture, it can be isolated as 5-½THF in 3% yield as a by-product in the synthesis of complex 4.



Scheme 3. Synthesis of Intermediates **5** and **6**.

The structure of dinuclear species **6** was established by single-crystal X-ray diffraction (Figure 2). Surprisingly, apart from CO ligands derived from the alcohol, the complex contains a bridging butyrate anion, itself the product of 1-butanol oxidation. NMR and MALDI-MS data on complexes **5** and **6** necessitate them to be diastereomers. Identical composition of the cations in **5** and **6** was deduced from the mass spectra showing molecular ion peaks at m/z 857.01 and 857.21 Da, respectively. While **6** has a reflection plane and contains two chemically equivalent PN ligands, complex **5** has lower symmetry, generating two sets of peaks for two different PN ligands in ¹H NMR spectrum. Based on this, we formulate **5** and **6** as *trans*- and *cis*-isomers due to the arrangement of the PN ligands (Figure 3). Consequently, their respec-

tive bridging hydride ligands have different coupling patterns in 1 H NMR spectra: a doublet of doublets in **5** ($^{2}J_{trans-PH}$ = 44.7 Hz and $^{2}J_{cis-PH}$ = 12.5 Hz) and a triplet in **6** ($^{2}J_{cis-PH}$ = 10.2 Hz).

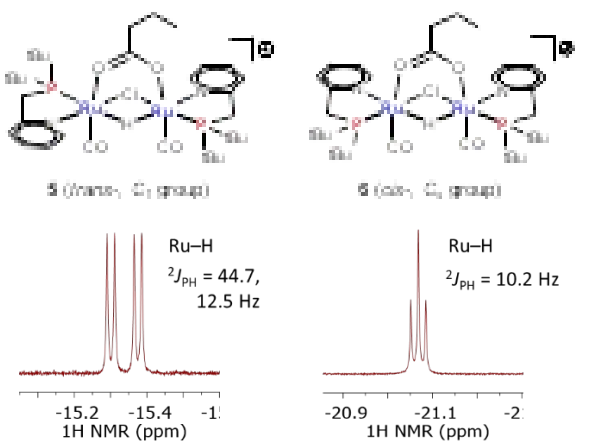
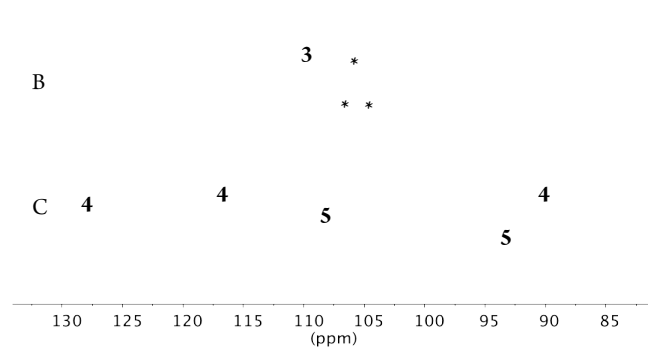


Figure 3. Coupling Patterns of the Hydride Ligands in ¹H NMR Spectra of Diastereomers **5** and **6**.

Mechanism of Precatalyst Evolution and Death

We conducted a series of additional experiments to investigate reactivity of 3-6 and determine the factors that govern their formation in the catalytic reaction. The results of these studies can be formulated in the following 5 points.

- 1. Complex 4 preferentially forms at high ruthenium loading. Formation of 4 depends on the $[HexNH_2]/[Ru]$ ratio in the reaction, and the complex is detected only when $[HexNH_2]/[Ru] < 40$ (e.g., Ru loading must be higher than 2.5 mol% for 4 to form). Under typical catalytic conditions, the catalyst loading is below 1 mol%, so complex 4 is not readily formed.
- 2. Complex 4 forms from 1 and 3 through respectively dinuclear and trinuclear intermediates. It appears that generation of trinuclear complex 4 from mononuclear species 1 and 3 proceeds through the intermediacy of a dinuclear species. To look for a possible dinuclear intermediate, we terminated the catalytic reaction ([1]:[HexNH₂]:[BuOH] is 1: 6.5: 144) after 10 minutes. We find a ³¹P NMR spectrum from this experiment that contains peaks of 1, 3, and 4, in addition to three new signals at 106.19, 105.65, and 104.57 ppm (Figure 4B). We chromatographically separated the new catalytic intermediates and analyzed them by MALDI-MS. The major components were identified as a dinuclear (785.22 Da) and a trinuclear (1193.76 Da) complexes, which undergo complete transformation to 4 within 30 min (Figures 4C and S23). Unfortunately, we could not obtain sufficient data to establish the structures and stabilities of the new species, hereinafter referred to as complex 4 predecessors.



A

Figure 4. ³¹P{¹H} NMR Spectra of Ruthenium Species Formed after 3 min (A), 10 min (B), and 30 min (C). Species of Unknown Structure are Marked with Asterisks.

3. None of complexes 3-6 is the catalyst resting state. After preparing samples of 3-6 we wanted to know if any of these could be the catalyst resting state in amine-alcohol coupling. For this purpose, we compared catalytic activity of 1 and 3-6 in the reaction between 1-aminohexane and alcohols (Table 3). As expected, pre-catalyst 1 gives full conversion of 1-aminohexane, as one would anticipate if the resting catalyst were added directly to the reaction. None of the remaining complexes gives an analogous result: they all either suffer from poor activity (complexes 3 and 4) or have no activity at all (complexes 5 and 6). Full conversion of 1-aminohexane is achieved when the mixture of complex 4 predecessors is used, indicating that one of the components is (or can access) the catalyst resting state (entry 8). Thus, we term complex 4 as a dormant form of the catalyst, whereas inactivity of 5 and 6 makes them ultimate, dead forms.

Table 3. Catalytic Activity Comparison Test.^a

/	\sim NH ₂	[Ru] (1 m	nol%)	NHR		
	ROH	110 °C,	18 h	\sim NR ₂		
Entry	[Ru]	R	HexNH ₂ , % ^b	HexNHR, %	HexNR ₂ , %	
1	1	PhCH ₂	0	> 99	0	
2	1	Bu	0	52	48	
3	3	PhCH ₂	6	73	0	
4	4	PhCH ₂	55	28	0	
5	4	Bu	32	68	0	
6	5	Bu	100	0	0	
7	6	Bu	100	0	0	
8	see text	Bu	0	85	15	

 $^{\rm a}$ Reaction conditions: a mixture of 1-aminohexane (51 mg, 0.5 mmol), benzyl alcohol (81 mg, 0.75 mmol) and Ru complex (5.00 x 10^6 mol of Ru atoms) was stirred in a closed reactor at 110 °C for 18 h. $^{\rm b}$ The yields were calculated from $^{\rm l}$ H NMR spectra.

4. Complex 4 forms when primary amine is consumed, and the catalytic reaction is over. Whereas it is formed at 110 °C with a good yield, complex 4 should be quite stable under the catalytic conditions. Indeed, it does not react with H₂, CO, and/or CO₂ in CH₂Cl₂ solution at 1 atm; no change is observed upon its treatment with 1-butanol or 1-aminohexane independently at 110 °C over 24 hours. When 4 is heated with both 1-butanol and 1-aminohexane, however, it undergoes full conversion to a diversity of species within 7 hours (Figure S24). Also, 'H NMR analysis of organic materials formed in the catalytic reaction shows absence of 1-aminohexane when complex 4 begins to form. This correlation shows limited compatibility of 4 and the primary

amine and renders 4 a kinetically stable product of post-catalytic transformations.

5. Complex 4 reacts slowly with a secondary amine and water to form the ultimate dead species 5 and 6. Why does the catalyst die? Since complex 4 begins to form as soon as alcohol-amine coupling is complete, the subsequent slow transformations of dormant catalyst 4 to the terminal (dead) forms 5 and 6 should be taking place in the medium of 1-(butylamino)hexane, water, and 1-butanol. Indeed, when complex 4 reacts directly with 1-(butylamino)hexane, water, and 1-butanol (110 °C, 20 h), complexes 5 and 6 are formed, as shown by a ¹H NMR experiment (Figure S24). This process does not affect product yields in alcohol-amine coupling when precatalyst loading is higher than 50 ppm. However, catalyst deactivation becomes a problem at lower catalyst loading (below 50 ppm), where a smaller portion of catalyst is available to be sacrificed to destructive interaction with reaction byproducts.

In contrast to formation of complex **4**, generation of **5** and **6** is independent of the system's [HexNH₂]/[Ru] ratio. The bridging butyrate ligand in **5** and **6** emerges from ruthenium-catalyzed acceptorless dehydrogenation of butanol to butyrate, which is well known. ^{38–46} Typically, the reaction requires hydroxide as a source of oxygen (Scheme 4A), however, in our case combination of water and secondary amine seems sufficient (Scheme 4B). We find that 1-butanol oxidation happens stoichiometrically rather than catalytically, since we did not detect free butyrate in the reaction mixture.

A R
$$^{\wedge}$$
OH + OH $^{\bullet}$ $\xrightarrow{\text{[Ru]}}$ $\xrightarrow{\text{Ru}}$ $\xrightarrow{\text{Ru}}$ $\xrightarrow{\text{Ru}}$ + 24.
B R $^{\wedge}$ OH + HO + RNH $\xrightarrow{\text{[Ru]}}$ $\xrightarrow{\text{Ru}}$ $\xrightarrow{\text{Ru}}$ $\xrightarrow{\text{Ru}}$ RNH, + 24.

Scheme 4. Ruthenium-Catalyzed Alcohol Oxidation.

Considering these points, we propose below a unified scheme for precatalyst activation, evolution, and death (Scheme 5). The process begins with substitution of chloride for butoxide in precatalyst 1, this requires equimolar amounts of 1-butanol and 1-aminohexane, where the amine is an HCl scavenger. The resulting butoxide complex 1-**OBu** undergoes rapid β-hydride elimination to form butanal and hydride complex 3. We have not observed 1-OBu directly, but its intermediacy is required for the formation of 3. Following transformations of 3 include p-cymene dissociation, selective carbonylation of one of the metals, and dimerization through ortho-metalation of a pyridine fragment. We propose that the resulting dinuclear species 7 of unknown structure could be the active catalyst, and a predecessor of complex 4. At high ruthenium loading, when catalytic reaction is complete, unreacted 1 can trap the dinuclear active catalyst 7 to form trinuclear dormant 4. The process is fast and selective due to high kinetic stability of 4. Then, the system slowly reaches thermodynamic rest through a reaction among 4, 1-(butylamino)hexane, water, and 1-butanol to form the dead catalyst forms 5 and 6.

Scheme 5. Precatalyst Activation and Death.

Discovery of the trinuclear ruthenium cluster 4 illustrates the high complexity of the inorganic side of our catalytic story. It is a wellknown phenomenon that ruthenium, 47,48 osmium, 48 and iridium 49,50 halide complexes can consecutively dehydrogenate and decarbonylate primary alcohols in the presence of a phosphine ligand, giving rise to M-CO fragment. This is the reason for carbonyl ligand being present in 4 - 6 and some other metal complexes, that are catalytically competent in alcohol dehydrogenation. Scheme 6 demonstrates generation of such complexes and highlights their common fragment (PN)MH(CO) $(M = Ru^{II})$ and Ir^{III} . This structural analogy appears to be a consequence of the thermodynamic stability of (PN)MH(CO) fragments, this allows them to form and be stable under catalytic reaction conditions (Scheme 6B and 6C).27 We believe that selective monocarbonylation in all these cases is the crucial step in precatalyst evolution to the active catalyst. We are presently working to test this hypothesis.

Scheme 6. Formation of Structurally Related Catalytic Complexes.

Electrochemistry

Triruthenium clusters are known to exhibit rich redox chemistry. 51-54 Because we were concerned that single-electron transformations of 4 could be causing important events in our catalyst lifecycle that would be invisible by NMR, we thought it prudent to determine whether 4 has facile 1-electron redox transitions and whether these transitions are reversible and/or their products are stable.

Redox properties of $4 (Ru_3^+)$ were investigated by cyclic voltammetry in 0.1 M CH_2Cl_2 solution of $[Bu_4N]PF_6$ at ambient temperature.

Overall, four redox events were detected in the potential range of -2.0 to $1.7~\rm V\,vs.~Fc^+/Fc.$ Upon scanning cathodically, the first reduction occurs at $E_{1/2}=-0.784~\rm V.$ This redox event is electrochemically irreversible ($\Delta E_{\rm p}=213~\rm mV)$), and the back feature appears only at scan rates higher than 400 mV/s. Applying more negative potential causes the second reduction event at $E_{\rm p}=-1.776~\rm V$ (at $100~\rm mV/s$). The corresponding back feature is not observed even at high scan rates. Thus, the products of both reduction steps are unstable in the solution, making these events chemically irreversible.

Applying positive potential, Ru3+ undergoes electrochemically reversible one electron oxidation to Ru₃²⁺ at $E_{1/2} = 0.442 \text{ V} (\Delta E_p = 63)$ mV) (Figure 5). Variable scan rate study showed that Ru₃²⁺/Ru₃⁺ couple obeys the Randles-Sevcik equation and, therefore, Ru₃²⁺ and Ru₃⁺ are freely diffusing in the solution. The second oxidation event occurs at $E_p = 1.481 \text{ V}$ (at 100 mV/s), it is irreversible because of subsequent chemical transformation. Electrochemical reversibility of the first oxidation step indicates possibility for chemical oxidation of complex 4 using an oxidant with the formal potential higher than 0.442 V. For example, oxidation with AgOTf ($E_{Ag+/Ag} = 0.65 \text{ V}$)55 in CH_2Cl_2 solution followed by crystallization from THF gives [Ru₃](OTf)₂·THF (8·THF) in 73% yield. Composition of the product was established by elemental analysis. Effective magnetic moment (μ_{eff}) of 8 was measured in CD₂Cl₂ solution by Evans method^{56,57} using a change of CH₂Cl₂ chemical shift and found to be 1.88 BM. This value corresponds to one unpaired electron in Ru₃²⁺ and is slightly higher than the spin-only value (1.73 BM) for $S = \frac{1}{2}$ state.

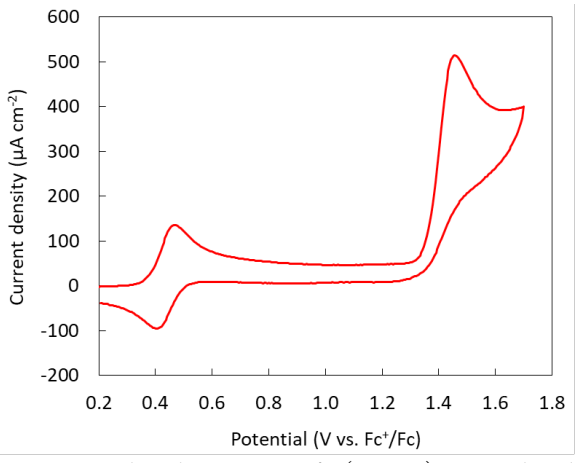


Figure 5. Cyclic voltammogram of 4 (1.0 mM) in CH_2Cl_2 with 0.1 M [Bu₄N]PF₆ at a scan rate of 50 mV/s.

Based on high positive potential of $\mathrm{Ru_3}^{2+}/\mathrm{Ru_3}^+$ couple, we believe that we are not generating a persistent concentration of a paramagnetic metal species in our catalytic reaction. In sum, we find that these observed electrochemical potentials and magnetic moments, although interesting in their own right, are inconsistent with any species that we observed in the catalytic pathway.

SUMMARY

In conclusion, we have demonstrated the utility of complex ${\bf 1}$ as a precatalyst for alcohol-amine coupling of aliphatic and some heterocyclic carbinol substrates. Detailed analysis of the catalytic reaction between 1-butanol and 1-aminohexane unraveled the precatalyst evolution sequence, that involves complexes ${\bf 3}-{\bf 6}$. Complex ${\bf 4}$ is a kinetically stable dormant catalyst form, whereas complexes ${\bf 5}$ and ${\bf 6}$ are the ultimate dead catalyst forms. Selective formation of ${\bf 4}$ is facilitated by a high ruthenium loading (> 2.5 mol% Ru) and forms via trapping a dinuclear active catalyst with unreacted precatalyst. Exhaustive catalyst poi-

soning is caused by the reaction with secondary amine, alcohol, and water to give $\mathbf{5}$ and $\mathbf{6}$. For the first time, we reveal the inherence of MH(CO) fragment to alcohol dehydrogenation catalysts, that is generated from an alcohol during precatalyst activation.

EXPERIMENTAL SECTION

Materials and Methods. Complex 1 was synthesized according to published procedure.21 CDCl3 and CD2Cl2 were purchased from Cambridge Isotope Laboratories and were dried and distilled over CaH₂. All alcohols and amines were purchased from commercial sources and were dried and distilled over CaH, as well. Tyramine was sublimed in vacuum. Hexane, CH2Cl2, Et2O, and THF were dried using a solvent purification system. HPLC grade hexane and ethyl acetate (EDM Millipore) were used without purification for chromatographic isolation of A - F on Teledyne CombiFlash instrument with "RediSep Rf Gold Amine" columns. All reactions were conducted under nitrogen either in a Vacuum Atmospheres glovebox (0-5 ppm O₂ for all manipulations) or outside the glovebox in a closed reactor. ¹H, ¹³C, ¹⁹F, and ³¹P NMR spectra were acquired on Varian Mercury 400, VNMRS-500, and VNMRS-600 spectrometers and processed using MestReNova 12.0.1. All chemical shifts are reported in ppm and referenced to the residual ¹H or ¹³C solvent peaks. Following abbreviations are used: (s) singlet, (bs s) broad singlet, (d) doublet, (t) triplet, (dd) doublet of doublets, etc. NMR spectra of all metal complexes were taken in 8" J. Young tubes (Wilmad or Norell) with Teflon valve plugs. GC-MS analyses were performed on Thermo Scientific Focus DSQ II instrument. MALDI-MS spectra were acquired on Bruker Autoflex Speed MALDI Mass Spectrometer. Elemental analyses were conducted on Flash 2000 CHNS Elemental Analyzer. Infrared spectra were recorded on Bruker OPUS FTIR spectrometer. Electronic absorption spectra were acquired on Perkin-Elmer UV-Vis-NIR spectrometer. Cyclic voltammetry experiments were carried out using a Pine potentiostat in a single compartment cell under nitrogen.

General Procedure for Coupling of Amines and Alcohols. A mixture of primary amine (2.0 mmol), alcohol, and complex 1 (see table 2) was stirred for required period in a closed reactor at 110 °C. Then, all volatile components were removed under vacuum, and the product was purified by flash column chromatography (SiO $_2$) hexane/ethyl acetate gradient).

1-(Butylamino)hexane (**A**). Yellow oil (0.28 g, 90%). ¹H NMR (400 MHz, CDCl₃): δ 2.58 (t, J = 7.3 Hz, 2H, CH₂), 2.57 (t, J = 7.3 Hz, 2H, CH₂), 1.52 – 1.40 (m, 4H, 2CH₂), 1.38 – 1.21 (m, 8H, 4CH₂), 1.04 (br s, 1H, NH), 0.94 – 0.84 (m, 6H, 2CH₃). ¹³C NMR (101 MHz, CDCl₃): δ 50.34, 49.98, 32.49, 31.95, 30.33, 27.25, 22.76, 20.68, 14.18, 14.16. IR (PE film, cm⁻¹): 2927, 1467, 1131, 892. GC-MS: m/z calcd. for [C₁₀H₂₃N]⁺ 157.18, found 157.15.

4-(2-(Butylamino)ethyl)phenol (**B**). Colorless crystals (0.27 g, 70%). ¹H NMR (500 MHz, CDCl₃): δ 7.03 (d, J = 8.2 Hz, 2H, ArH), 6.71 (d, J = 8.2 Hz, 2H, ArH), 4.26 (br s, 2H, NH, OH), 2.88 (t, J = 6.8 Hz, 2H, CH₂), 2.75 (t, J = 6.8 Hz, 2H, CH₂), 2.64 (t, J = 7.4 Hz, 2H, CH₂), 1.47 (p, J = 7.5 Hz, 2H, CH₂), 1.29 (h, J = 7.0 Hz, 2H, CH₂), 0.88 (t, J = 7.3 Hz, 3H, CH₃). ¹³C NMR (126 MHz, CDCl₃): δ 155.55, 130.46, 129.86, 115.93, 50.98, 49.48, 34.91, 31.78, 20.59, 14.06. IR (KBr, cm⁻¹): 1618, 1598, 1520, 1465, 1379, 1255, 1109, 831. MALDI-MS: m/z calcd. for $[C_{12}H_{20}NO]^+$ 194.15, found 194.44.

N-(3,4-Dimethoxyphenethyl)butan-1-amine (C). Yellow oil (0.39 g, 83%). ¹H NMR (600 MHz, CDCl₃): δ 6.82 – 6.78 (m, 1H, ArH), 6.76 – 6.72 (m, 2H, ArH), 3.86 (s, 3H, OMe), 3.85 (s, 3H, OMe), 2.85 (t, J = 7.1 Hz, 2H, CH₂), 2.75 (t, J = 7.1 Hz, 2H, CH₂), 2.61 (t, J = 7.4 Hz, 2H, CH₂), 1.44 (p, J = 7.2 Hz, 2H, CH₂), 1.31 (h, J = 7.7 Hz,

2H, CH₂), 0.89 (t, J = 7.4 Hz, 3H, CH₃). ¹³C NMR (151 MHz, CDCl₃): δ 149.02, 147.53, 132.91, 120.66, 112.12, 111.45, 56.05, 55.94, 51.53, 49.81, 36.15, 32.41, 20.63, 14.14. IR (PE film, cm⁻¹): 1594, 1519, 1466, 1421, 1264, 1240, 1159, 1143, 1033, 809, 766. MALDI-MS: m/z calcd. for $[C_{14}H_{24}NO_2]^+$ 238.18, found 238.64.

2-(2-(Butylamino)ethyl)pyridine (**D**). Yellow oil (0.29 g, 81%). 1 H NMR (600 MHz, CDCl₃): δ 8.50 (d, J = 4.8 Hz, 1H, ArH), 7.55 (td, J = 7.6, 1.8 Hz, 1H, ArH), 7.14 (d, J = 7.8 Hz, 1H, ArH), 7.08 (ddd, J = 7.5, 4.9, 0.9 Hz, 1H, ArH), 3.01 – 2.92 (m, 4H, 2CH₂), 2.60 (t, J = 7.3 Hz, 2H, CH₂), 1.43 (p, J = 7.3 Hz, 2H, CH₂), 1.29 (h, J = 7.6 Hz, 3H, NH, CH₂), 0.86 (t, J = 7.4 Hz, 3H, CH₃). 13 C NMR (151 MHz, CDCl₃): δ 160.52, 149.48, 136.40, 123.36, 121.28, 49.72, 49.62, 38.75, 32.38, 20.59, 14.10. IR (PE film, cm⁻¹): 1594, 1573, 1476, 1438, 1130, 751. GC-MS: m/z calcd. for $[C_{11}H_{18}N_2]^+$ 178.15, found 178.10.

3-(2-(Hexylamino)ethyl)thiophene (E). Colorless oil (0.17 g, 62%). ¹H NMR (500 MHz, CDCl₃): δ 7.30 – 7.24 (m, 1H, ArH), 7.03 – 6.94 (m, 2H, ArH), 2.92 – 2.80 (m, 4H, 2CH₂), 2.61 (t, J = 7.3 Hz, 2H, CH₂), 1.46 (p, J = 7.0 Hz, 2H, CH₂), 1.37 – 1.22 (m, 6H, 3CH₂), 1.04 (br s, 1H, NH), 0.88 (t, J = 6.6 Hz, 3H, CH₃). ¹³C NMR (126 MHz, CDCl₃): δ 140.62, 128.31, 125.65, 120.99, 50.55, 50.07, 31.91, 30.99, 30.24, 27.18, 22.75, 14.18. IR (PE film, cm⁻¹): 1732, 1464, 1129, 774. MALDI-MS: m/z calcd. for $[C_{12}H_{22}NS]^+$ 212.15, found 212.51.

3-(2-(Butylamino)ethyl)indole (**F**). Yellow solid (0.32 g, 74%). 1 H NMR (600 MHz, CDCl₃): δ 8.66 (br s, 1H, NH), 7.60 (d, J = 7.9 Hz, 1H, ArH), 7.35 (d, J = 8.1 Hz, 1H, ArH), 7.16 (t, J = 7.6 Hz, 1H, ArH), 7.08 (t, J = 7.5 Hz, 1H, ArH), 7.01 (s, 1H, ArH), 3.90 (br s, 1H, NH), 3.09 (t, J = 7.2 Hz, 2H, CH₂), 3.01 (t, J = 7.2 Hz, 2H, CH₂), 2.69 (t, J = 7.8 Hz, 2H, CH₂), 1.54 (p, J = 7.6 Hz, 2H, CH₂), 1.28 (h, J = 7.4 Hz, 2H, CH₂), 0.86 (t, J = 7.4 Hz, 3H, CH₃). 13 C NMR (151 MHz, CDCl₃): δ 136.55, 127.29, 122.59, 122.09, 119.39, 118.76, 112.48, 111.45, 49.21, 48.90, 30.67, 24.52, 20.41, 13.90. IR (KBr, cm $^{-1}$): 3289, 2729, 1626, 1456, 1358, 1237, 1107, 748. MALDI-MS: m/z calcd. for $[C_{14}H_{11}N_2]^+$ 217.17, found 217.52.

 $[\mathbf{Ru}(\mathbf{OTf})(\eta^6 - \mathbf{C}_{10}\mathbf{H}_{14})(\mathbf{PyCH}_2\mathbf{PBu}_2^{\mathsf{t}})]\mathbf{OTf}(\mathbf{2})$. Complex 1 (100 mg, 1.54 x 10⁻⁴ mol) and AgOTf (39 mg, 1.54 x 10⁻⁴ mol) were stirred in CH₂Cl₂ (4 mL) for 1 hour at 25 °C. Then, the solution was filtered and treated with Et₂O (10 mL) to induce crystallization of the product. Orange flakes were filtered, washed with Et₂O, and dried in vacuum (108 mg, 92%). ¹H NMR (500 MHz, CD₂Cl₂): δ 9.52 (d, J = 5.9 Hz, 1H, Py), 7.93 (t, J = 7.9 Hz, 1H, Py), 7.60 - 7.45 (m, 2H, Py), 6.70 (d, I = 6.4 Hz, 1H, C_6H_4), 6.65 (d, I = 5.5 Hz, 1H, C_6H_4), 6.48 (d, I = 6.4Hz, 1H, C_6H_4), 5.84 (d, J = 5.9 Hz, 1H, C_6H_4), 3.47 (dd, J = 16.9, 13.9 Hz, 1H, CH₂), 3.13 (dd, J = 16.8, 7.9 Hz, 1H, CH₂), 2.76 (hept, J = 7.0Hz, 1H, Prⁱ), 2.13 (s, 3H, CH₂), 1.51 (d, J = 14.6 Hz, 9H, Bu^t), 1.34 (d, $J = 6.8 \text{ Hz}, 3H, Pr^i), 1.31 - 1.23 \text{ (m, 12H, Pr}^i, Bu}^i).$ ¹³C{¹H} NMR (151 MHz, CD_2Cl_2): δ 164.3 (d, J = 3.2 Hz), 158.5, 141.7, 125.5, 125.1 (d, *J* = 8.6 Hz), 106.3, 99.7, 93.7, 89.7, 87.6, 81.7, 38.9 (m), 32.2 (d, J = 21.1 Hz), 31.4, 30.2 (d, J = 2.6 Hz), 30.0 (d, J = 2.4 Hz), 23.9,21.3, 18.6. ³¹P{¹H} NMR (202 MHz, CD₂Cl₂): δ 90.65. ¹⁹F NMR (564 MHz, CD₂Cl₂): δ –78.66 (s, 3F, RuOTf), –78.82 (s, 3F, TfO⁻²). IR (KBr, cm⁻¹): 2978, 1613, 1479, 1330, 1274, 1234, 1204, 1163, 1003, 640, 518. MALDI-MS: *m/z* calcd [C₂₅H₃₈F₃NO₃PRuS]⁺ 622.13, found 622.28. Anal. calcd for C₂₆H₃₈F₆NO₆PRuS₂: C 40.52, H 4.97, N 1.82. Found: C 40.43, H 5.21, N 1.80.

[RuH(η^6 -C₁₀H₁₄)(PyCH₂PBu^t₂)]OTf (3). Complex 2 (100 mg, 1.30 x 10⁻⁴ mol) and 2-propanol (4 mL) were heated in a closed reactor at 110 °C for 1 hour. Then, the solvent was removed in vacuum (oil bath, 60 °C) to give a dark-yellow oil. Upon its crystallization from CH₂Cl₂-

Et₂O two fractions of crystals were obtained: orange unreacted complex 2 and yellow product 3. The crystals were filtered, washed with $Et_2O,$ and dried in vacuum (40 mg, 50%). 1H NMR (600 MHz, CD_3Cl_3): δ 8.64 (d, I = 5.8 Hz, 1H, Pv), 7.65 (t, I = 7.6 Hz, 1H, Pv), 7.38 (d, J = 7.8 Hz, 1H, Py), 7.11 (t, J = 6.7 Hz, 1H, Py), 5.91 (d, J =6.1 Hz, 1H, C_6H_4), 5.81 (d, J = 6.0 Hz, 1H, C_6H_4), 5.61 (d, J = 6.2 Hz, 1H, C_6H_4), 4.81 (d, J = 6.0 Hz, 1H, C_6H_4), 3.38 (dd, J = 16.9, 10.3 Hz, 1H, CH₂), 3.09 (dd, J = 16.9, 7.7 Hz, 1H, CH₂), 2.71 (hept, J = 6.8 Hz, 1H, Pr^{i}), 2.34 (s, 3H, CH_{3}), 1.34 (d, J = 7.0 Hz, 3H, Pr^{i}), 1.33 (d, J =7.0 Hz, 3H, Pr^{i}), 1.29 (d, J = 14.0 Hz, 9H, Bu^{t}), 1.25 (d, J = 13.2 Hz, 9H, Bu^t), -8.65 (d, ${}^{2}J_{PH}$ = 42.8 Hz, 1H, RuH). ${}^{13}C\{{}^{1}H\}$ NMR (151 MHz, CD_2Cl_2): δ 163.0 (d, J = 3.1 Hz), 157.6, 138.2, 124.0, 123.8 (d, J= 8.8 Hz), 117.8, 105.9, 95.4, 88.5, 87.9 (d, J = 6.5 Hz), 77.7, 38.2 (d, J = 6.5 Hz) = 10.7 Hz), 36.5 (d, J = 26.1 Hz), 35.7 (d, J = 24.8 Hz), 32.8, 30.3 (d, J = 24.8 Hz), 32.8, 30.3 (d, J = 24.8 Hz) = 3.1 Hz), 29.5 (d, J = 4.5 Hz), 24.7, 23.0, 19.7. ${}^{31}P{}^{1}H$ } NMR (243) MHz, CD₂Cl₂): δ 109.75 (d, J = 11.8 Hz). ¹⁹F NMR (564 MHz, CD₂Cl₂): δ –78.84. IR (KBr, cm⁻¹): 2976, 2023 (ν_{RuH}), 1477, 1281, 1265, 1154, 1034, 639. MALDI-MS: *m/z* calcd for [C₂₄H₃₉NPRu]⁺ 474.19, found 474.30. Anal. calcd for C₂₅H₃₉F₃NO₃PRuS: C 48.22, H 6.31, N 2.25. Found: C 48.33, H 6.37, N 2.23.

 $[Ru_{_{1}}H_{_{2}}Cl_{_{2}}(CO)(PyCH_{_{2}}PBu^{t}_{_{2}})_{_{2}}\{\mu\text{-}(C_{_{5}}H_{_{3}}N)CH_{_{2}}PBu^{t}_{_{2}}\}]OTf \quad (4).$ Complex 1 (2.00 g, 3.04 x 10⁻³ mol), 1-butanol (42 mL, 0.459 mol), and 1-aminohexane (1.54 g, 1.52 x 10⁻² mol) were stirred under N₂ in a closed reactor at 110 °C for 1 hour. The orange suspension turned dark-green. All volatile components were removed from the hot solution under vacuum. The evacuated reactor was transferred inside a glovebox. The remains of organic materials were extracted by trituration with hexane and then with Et₂O to give dark-green precipitate. It was filtered and washed with Et₂O. The material contains 4 and 5. The solid was recrystallized twice from CH₂Cl₂–Et₂O affording the product as black-green crystals (808 mg, 63%). Crystals suitable for X-ray analysis were obtained by slow evaporation of CH₂Cl₂–Et₂O solution. ¹H NMR (600 MHz, CD₂Cl₂): δ 8.64 (d, J = 5.4 Hz, 1H, Py), 8.30 (d, J = 5.7 Hz, 1H, Py), 7.71 (d, J = 7.8 Hz, 1H, Py), 7.62 (t, J = 7.5 Hz, 1H, Py), 7.29 (t, I = 7.4 Hz, 1H, Py), 7.24 (d, I = 7.5 Hz, 1H, Py), 6.90 (t, J = 6.5 Hz, 1H, Py), 6.80 - 6.70 (m, 3H, C₅H₃N, Py), 6.11 (d, J =7.7 Hz, 1H, C_5H_3N), 3.71 (dd, J = 16.7, 11.1 Hz, 1H, CH_7), 3.60 (dd, J= 17.3, 11.7 Hz, 1H, CH₂), 3.48 – 3.29 (m, 3H, CH₂), 3.07 (dd, J =16.6, 7.9 Hz, 1H, CH₂), 1.73 (d, J = 14.4 Hz, 9H, Bu^t), 1.34 (d, J = 13.4Hz, 9H, Bu^t), 1.23 (d, J = 12.7 Hz, 9H, Bu^t), 1.17 (d, J = 13.3 Hz, 9H, Bu^{t}), 0.96 (d, J = 13.5 Hz, 9H, Bu^{t}), 0.90 (d, J = 12.4 Hz, 9H, Bu^{t}), – 16.50 (ddd, ${}^{2}J_{PH}$ = 51.6, 27.3, 9.1 Hz, 1H, RuH), -21.36 (dd, ${}^{2}J_{PH}$ = 20.0, 4.5 Hz, 1H, RuH). ¹³C{¹H} NMR (151 MHz, CD₂Cl₂): δ 205.9 (d, J = 12.1 Hz), 189.0, 168.2, 165.6, 164.1 (d, J = 5.4 Hz), 156.8,154.6, 135.7, 133.8, 131.2, 130.1, 124.0 (d, *J* = 9.0 Hz), 122.3, 121.8 (d, J = 9.4 Hz), 121.6, 115.5 (d, J = 8.8 Hz), 38.3 (d, J = 18.4 Hz), 38.1 (d, J = 19.9 Hz), 37.2 (d, J = 11.0 Hz), 36.7 (d, J = 22.0 Hz), 35.5 (d, J = 22.0 Hz)= 19.8 Hz), 34.7 (d, J = 14.5 Hz), 34.5 (d, J = 11.3 Hz), 30.8, 30.7, 29.8, 29.1, 28.6, 28.5. ³¹P{¹H} NMR (243 MHz, CD₂Cl₂): δ 128.34, 116.38, 89.76. ¹⁹F NMR (564 MHz, CD₂Cl₂): δ –78.89. IR (KBr, cm⁻ 1): 2957, 2908, 2875, 1941 (ν_{CO}), 1273, 1035, 639. UV-Vis (CH₂Cl₂; λ_{max} , nm (ϵ , M⁻¹ cm⁻¹)): 293 (15772), 420 (16409), 586 (4362). MALDI-MS: m/z calcd for $[C_{43}H_{73}Cl_2N_3OP_3Ru_3]^+$ 1115.15, found 1114.71. Anal. calcd for C₄₄H₇₃Cl₂F₃N₃O₄P₃Ru₃S: C 41.80, H 5.82, N 3.32. Found: C 41.60, H 5.88, N 3.25.

trans-[$\mathbf{Ru_2HCl(CO)_2(PyCH_2PBut_2)_2(\mu-O_2CPr^n)}$] CI (5). A brown-yellow $\mathbf{CH_2Cl_2}$ -Et_2O solution, obtained in the synthesis of 4, was evaporated to dryness and treated with THF. Concentration of the resulting solution afforded yellow crystals of $\mathbf{5}$ -½THF. They were filtered, washed with THF, and dried in vacuum. Yellow crystalline pow-

der (57 mg, 3%). ¹H NMR (600 MHz, CD₂Cl₂): δ 9.01 (d, J = 5.4 Hz, 1H, Py), 8.98 (d, J = 5.4 Hz, 1H, Py), 7.96 - 7.88 (m, 2H, Py), 7.88 -7.80 (m, 2H, Py), 7.29 (t, J = 6.3 Hz, 1H, Py), 7.16 (t, J = 6.3 Hz, 1H, Py), 4.07 (dd, J = 16.7, 9.2 Hz, 1H, CH_2), 3.93 (dd, J = 16.8, 10.2 Hz, 1H, CH₂), 3.75 (dd, J = 16.6, 10.3 Hz, 1H, CH₂), 3.69 (dd, J = 16.7, = 15.8, 7.8 Hz, 1H, CH₂CO₂), 1.44 (d, I = 14.0 Hz, 9H, Bu^t), 1.40 (d, I = 14.0 Hz, 9H, Bu^t = 14.2 Hz, 9H, Bu^t), 1.38 (d, J = 14.0 Hz, 9H, Bu^t), 1.33 – 1.23 (m, 2H, CH_2), 1.18 (d, J = 13.6 Hz, 9H, Bu^t), 0.61 (t, J = 7.3 Hz, 3H, CH_3), – 15.34 (dd, ${}^{2}J_{PH}$ = 44.7, 12.5 Hz, 1H, RuH). ${}^{13}C\{{}^{1}H\}$ NMR (151 MHz, CD_2Cl_2): δ 204.01 (d, ${}^2J_{CP}$ = 12.9 Hz, CO), 203.69 (d, ${}^2J_{CP}$ = 15.0 Hz, CO), 186.34 (CO₂), 165.95 (d, J = 3.7 Hz), 163.45 (d, J = 1.6 Hz), 158.30, 155.46, 139.55, 139.42, 125.55 (d, *J* = 8.4 Hz), 124.78 (d, *J* = 8.4 Hz), 123.95, 123.47, 40.23, 37.92 (d, J = 22.4 Hz), 37.79 (d, J = 22.4 Hz) 18.7 Hz), 37.62 (d, J = 14.1 Hz), 37.38 (d, J = 17.0 Hz), 36.45 (d, J = 17.0 Hz) 20.9 Hz), 35.09 (d, J = 18.7 Hz), 30.07 (d, J = 2.6 Hz), 29.85 (d, J = 3.0 Hz)Hz), 29.50 (d, J = 2.7 Hz), 29.32 (d, J = 2.6 Hz), 19.31, 13.66. ${}^{31}P\{{}^{1}H\}$ NMR (243 MHz, CD₂Cl₂): δ 108.22, 93.26. IR (KBr, cm⁻¹): 2975, 2911, 2878, 1967 (ν_{CO}), 1937 (ν_{CO}), 1558 (ν_{COO}), 1478, 1432. MALDI-MS: m/z calcd for $[C_{34}H_{56}ClN_2O_4P_2Ru_2]^+$ 857.15, found 857.01. Anal. calcd for C₇₂H₁₂₀Cl₄N₄O₉P₄Ru₄: C 46.60, H 6.52, N 3.02. Found: C 46.21, H 6.48, N 2.97.

cis-[Ru,HCl(CO),(PyCH,PBut,),(µ-O,CPrn)]OTf (6). Complex 1 (200 mg, 3.04 x 10⁻⁴ mol), 1-butanol (4 mL, 0.044 mol), and 1-aminohexane (308 mg, 3.04 x 10⁻³ mol) were stirred under N₂ in a closed reactor at 110 °C for 24 hours. The orange suspension turned brown. All volatile components were removed from the hot solution under vacuum to give a brown paste containing 5 and 6. The following manipulations were performed inside a glovebox. To enable crystallization of 6, organic and Ru-containing by-products were separated by column chromatography on "RediSep Rf reversed-phase C18" silica dried in an oven at 120 °C. The reaction mixture was dissolved in CH₂Cl₂, filtered, and dry loaded on the sorbent. A column (d = 1.5 cm) was filled with the sorbent (10 mL) in Et₂O and the dry loaded mixture. Elution with Et₂O gave a yellow band containing mostly organic by-products. Then, elution with Et₂O-CH₂Cl₂ (9:1) gave another yellow band containing 5 and 6. The process was completed by washing the column with CH₂Cl₃ that gave the final portion of **5** and **6**. At this point a green-colored band of 4 should remain on the column. The Et₂O-CH₂Cl₂ and CH₂Cl₂ solutions were combined and after a few days the product crystallized as 6·CH₂Cl₂. The orange crystals were separated, washed with Et,O, and dried in vacuum (30 mg, 18%). Crystals suitable for X-ray analysis were obtained by slow evaporation of CH₂Cl₂-Et₂O solution. ¹H NMR (600 MHz, CD₂Cl₂): δ 9.06 (d, J = 5.8 Hz, 2H, Py), 7.93 (t, J = 8.0 Hz, 2H, Py), 7.73 (d, J = 7.9 Hz, 2H, Py), 7.33(t, J = 6.7 Hz, 2H, Py), 3.83 (dd, J = 16.8, 10.9 Hz, 2H, CH₂), 3.57 (dd, $J = 16.9, 8.5 \text{ Hz}, 2\text{H}, \text{CH}_2$, 2.16 (t, $J = 7.5 \text{ Hz}, 2\text{H}, \text{CH}_2$), 1.48 (d, J =14.2 Hz, 18H, 2Bu^t), 1.39 (h, J = 7.4 Hz, 2H, CH₂), 1.13 (d, J = 13.6Hz, 18H, 2Bu^t), 0.79 (t, J = 7.4 Hz, 3H, CH₃), -21.07 (t, ${}^{2}J_{PH} = 10.2$ Hz, 1H, RuH). ${}^{13}C\{{}^{1}H\}$ NMR (151 MHz, CD₂Cl₂): δ 202.8 (d, ${}^{2}J_{CP}$ = 17.3 Hz, CO), 186.6 (CO₂), 163.3, 155.8, 139.4, 124.3 (d, J = 8.2 Hz), 124.2, 40.6, 38.1 (d, *J* = 14.6 Hz), 37.6 (d, *J* = 22.7 Hz), 37.3 (d, *J* = 22.2 Hz), 30.5 (d, J = 2.7 Hz), 29.4 (d, J = 2.6 Hz), 19.6, 13.8. ${}^{31}P\{{}^{1}H\}$ NMR (243 MHz, CD₂Cl₂): δ 104.65 (d, I = 9.0 Hz). ¹⁹F NMR (564 MHz, CD₂Cl₂): δ -78.94. IR (KBr, cm⁻¹): 2974, 1975 (ν _{CO}), 1944, 1559 (v_{COO}), 1283, 1262, 1027, 633. MALDI-MS: m/z calcd for $[C_{34}H_{56}ClN_2O_4P_2Ru_2]^+$ 857.15, found 857.21.

[Ru₃H₂Cl₂(CO)(PyCH₂PBu^t₂)₂{(C₅H₃N)CH₂PBu^t₂}](OTf)₂ (8). Complex 4 (20 mg, 1.58 x 10^{-5} mol) and AgOTf (5 mg, 1.94 x 10^{-5} mol) were stirred in CH₂Cl₂ (4 mL) for 1 hour at 25 °C. Dark-green

solution turned dark-blue, then it was filtered. The solvent was removed in vacuum giving a blue oil. It was dissolved in THF (2 mL) and shortly after the product crystallized as **8**·THF. It was filtered, washed with THF, then with hexane, and dried in vacuum. Black crystalline powder (16 mg, 73%). IR (KBr, cm⁻¹): 2961, 1971 (ν_{CO}), 1820, 1479, 1436, 1277, 1157, 1034, 828, 639. UV-Vis (CH₂Cl₂; λ_{max} , nm (ϵ , M⁻¹ cm⁻¹)): 305 (14043), 357 (9165), 605 (4465), 730 (3629). MALDI-MS: m/z calcd for [C₄₃H₇₃Cl₂N₃OP₃Ru₃]+ 1115.15, found 1114.72. Anal. calcd for C₄₉H₈₁Cl₂F₆N₃O₈P₃Ru₃S₂: C 39.62, H 5.50, N 2.83. Found: C 39.99, H 5.54, N 2.77.

ASSOCIATED CONTENT

Supporting Information.

The Supporting Information is available free of charge on the ACS Publications website at DOI: $10.1021/^{**}$.

Experimental procedures, characterization, and X-ray data (PDF)

Crystallographic data for 4 (CIF)

Crystallographic data for 6 (CIF)

AUTHOR INFORMATION

Corresponding Author

*E-mail for T.J.W.: travisw@usc.edu

ORCID

Valeriy Cherepakhin: 0000-0003-1966-9794 Travis J. Williams: 0000-0001-6299-3747

Notes

While complex 1 is commercially available from TCI, the authors receive no royalties from its sale and thus declare no competing financial interest.

ACKNOWLEDGMENTS

This work is sponsored by the NSF (CHE-1856395), and the Hydrocarbon Research Foundation. We thank the NSF (DBI-0821671, CHE-0840366, CHE-1048807) and NIH (1 S10 RR25432) for sponsorship of research instrumentation. V.C. acknowledges Sonosky fellowship support from the USC Wrigley Institute for Environmental Studies. We thank Prof. Ralf Haiges for help with X-ray crystallography. We are grateful to the Smaranda Marinescu group for providing equipment for electrochemical studies.

REFERENCES

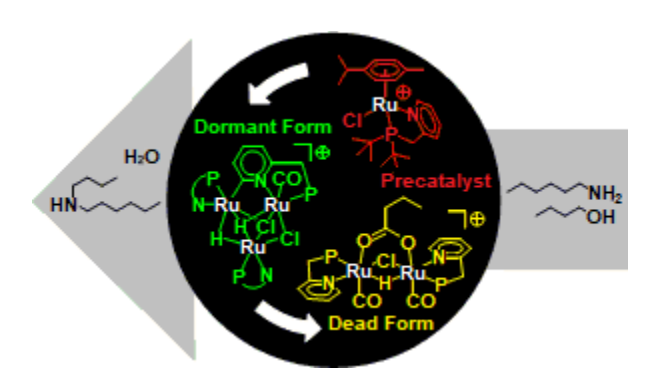
- Peña-López, M.; Neumann, H.; Beller, M. (Enantio)Selective Hydrogen Autotransfer: Ruthenium-Catalyzed Synthesis of Oxazolidin-2-Ones from Urea and Diols. *Angew. Chemie Int. Ed.* 2016, 55 (27), 7826–7830.
- (2) Zhang, M.; Imm, S.; Bähn, S.; Neumann, H.; Beller, M. Synthesis of α-Amino Acid Amides: Ruthenium-Catalyzed Amination of α-Hydroxy Amides. Angew. Chemie Int. Ed. 2011, 50 (47), 11197–11201.
- (3) Bähn, S.; Imm, S.; Mevius, K.; Neubert, L.; Tillack, A.; Williams, J. M. J.; Beller, M. Selective Ruthenium-Catalyzed N-Alkylation of Indoles by Using Alcohols. Chem. - A Eur. J. 2010, 16, 3590–3593.
- (4) Tillack, A.; Hollmann, D.; Mevius, K.; Michalik, D.; Bähn, S.; Beller, M. Salt-Free Synthesis of Tertiary Amines by Ruthenium-Catalyzed Amination of Alcohols. European J. Org. Chem. 2008, 2008 (28), 4745–4750.
- (5) Tillack, A.; Hollmann, D.; Michalik, D.; Beller, M. A Novel Ruthenium-Catalyzed Amination of Primary and Secondary Alcohols. *Tetrahedron Lett.* 2006, 47 (50), 8881–8885.
- (6) Broomfield, L. M.; Wu, Y.; Martin, E.; Shafir, A. Phosphino-Amine (PN) Ligands for Rapid Catalyst Discovery in Ruthenium-Catalyzed Hydrogen-Borrowing Alkylation of Anilines: A Proof of Principle. Adv. Synth. Catal. 2015, 357 (16–17), 3538–3548.
- (7) Leonard, J.; Blacker, A. J.; Marsden, S. P.; Jones, M. F.; Mulholland, K. R.; Newton, R. A Survey of the Borrowing Hydrogen Approach to the

- Synthesis of Some Pharmaceutically Relevant Intermediates. *Org. Process Res. Dev.* **2015**, *19* (10), 1400–1410.
- (8) Peishan, S.; Dang, T. T.; Seayad, A. M.; Ramalingam, B. Reusable Supported Ruthenium Catalysts for the Alkylation of Amines by Using Primary Alcohols. ChemCatChem 2014, 6 (3), 808–814.
- (9) Enyong, A. B.; Moasser, B. Ruthenium-Catalyzed N-Alkylation of Amines with Alcohols under Mild Conditions Using the Borrowing Hydrogen Methodology. J. Org. Chem. 2014, 79 (16), 7553–7563.
- (10) Maxwell, A. C.; Watson, A. J. A.; Hamid, M. H. S. A.; Williams, J. M. J.; Maytum, H. C.; Lamb, G. W.; Allen, C. L. Ruthenium-Catalyzed N-Alkylation of Amines and Sulfonamides Using Borrowing Hydrogen Methodology. J. Am. Chem. Soc. 2009, 131, 1766–1774.
- (11) Watson, A. J. A.; Maxwell, A. C.; Williams, J. M. J. Borrowing Hydrogen Methodology for Amine Synthesis under Solvent-Free Microwave Conditions. J. Org. Chem. 2011, 76 (7), 2328–2331.
- (12) Hamid, M. H. S. A.; Williams, J. M. J. Ruthenium Catalysed N-Alkylation of Amines with Alcohols. Chem. Commun. 2007, 43 (7), 725–727.
- (13) Hamid, M. H. S. A.; Williams, J. M. J. Ruthenium-Catalysed Synthesis of Tertiary Amines from Alcohols. *Tetrahedron Lett.* 2007, 48 (47), 8263– 8265.
- (14) Jumde, V. R.; Gonsalvi, L.; Guerriero, A.; Peruzzini, M.; Taddei, M. A Ruthenium-Based Catalytic System for a Mild Borrowing-Hydrogen Process. European J. Org. Chem. 2015, 2015 (8), 1829–1833.
- (15) Dang, T. T.; Ramalingam, B.; Seayad, A. M. Efficient Ruthenium-Catalyzed N-Methylation of Amines Using Methanol. ACS Catal. 2015, 5 (7), 4082–4088.
- (16) Monrad, R. N.; Madsen, R. Ruthenium-Catalysed Synthesis of 2- and 3-Substituted Quinolines from Anilines and 1,3-Diols. Org. Biomol. Chem. 2011, 9 (2), 610–615.
- (17) Marichev, K. O.; Takacs, J. M. Ruthenium-Catalyzed Amination of Secondary Alcohols Using Borrowing Hydrogen Methodology. ACS Catal. 2016, 6 (4), 2205–2210.
- (18) Huynh, H. V.; Gnanaprakasam, B.; Ramalingam, B.; Shan, S. P.; Seayad, A. M.; Dang, T. T.; Xiaoke, X. Benzimidazolin-2-Ylidene N-Heterocyclic Carbene Complexes of Ruthenium as a Simple Catalyst for the N-Alkylation of Amines Using Alcohols and Diols. RSC Adv. 2014, 5 (6), 4434–4442.
- (19) Fernández, F. E.; Puerta, M. C.; Valerga, P. Ruthenium(II) Picolyl-NHC Complexes: Synthesis, Characterization, and Catalytic Activity in Amine N-Alkylation and Transfer Hydrogenation Reactions. Organometallics 2012, 31 (19), 6868–6879.
- (20) Dubey, P.; Gupta, S.; Singh, A. K. Complexes of Pd(II), H6-C6H6Ru(II), and H5-Cp*Rh(III) with Chalcogenated Schiff Bases of Anthracene-9-Carbaldehyde and Base-Free Catalytic Transfer Hydrogenation of Aldehydes/Ketones and N -Alkylation of Amines. Organometallics 2019, 38 (4), 944–961.
- (21) Celaje, J. J. A.; Zhang, X.; Zhang, F.; Kam, L.; Herron, J. R.; Williams, T. J. A Base and Solvent-Free Ruthenium-Catalyzed Alkylation of Amines. ACS Catal. 2017, 7 (2), 1136–1142.
- (22) Şahin, N.; Özdemir, N.; Gürbüz, N.; Özdemir, İ. Novel N-Alkylbenzimidazole-Ruthenium (II) Complexes: Synthesis and Catalytic Activity of N-Alkylating Reaction under Solvent-Free Medium. Appl. Organomet. Chem. 2019, 33 (2), 1–13.
- (23) Balaraman, E.; Srimani, D.; Diskin-Posner, Y.; Milstein, D. Direct Synthesis of Secondary Amines From Alcohols and Ammonia Catalyzed by a Ruthenium Pincer Complex. Catal. Letters 2015, 145 (1), 139–144.
- (24) Ramachandran, R.; Prakash, G.; Nirmala, M.; Viswanathamurthi, P.; Malecki, J. G. Ruthenium(II) Carbonyl Complexes Designed with Arsine and PNO/PNS Ligands as Catalysts for N-Alkylation of Amines via Hydrogen Autotransfer Process. J. Organomet. Chem. 2015, 791, 130–140
- (25) Oldenhuis, N. J.; Dong, V. M.; Guan, Z. From Racemic Alcohols to Enantiopure Amines: Ru-Catalyzed Diastereoselective Amination. J. Am. Chem. Soc. 2014, 136 (36), 12548–12551.
- (26) Agrawal, S.; Lenormand, M.; Martín-Matute, B. Selective Alkylation of (Hetero)Aromatic Amines with Alcohols Catalyzed by a Ruthenium Pincer Complex. Org. Lett. 2012, 14 (6), 1456–1459.
- (27) Cherepakhin, V.; Williams, T. J. Iridium Catalysts for Acceptorless Dehydrogenation of Alcohols to Carboxylic Acids: Scope and Mechanism. ACS Catal. 2018, 8 (5), 3754–3763.
- (28) Yan, T.; Feringa, B. L.; Barta, K. Direct N-Alkylation of Unprotected Amino Acids with Alcohols. Sci. Adv. 2017, 3, 1–8.
- (29) Imm, S.; Neubert, L.; Neumann, H.; Beller, M. An Efficient and General

- Synthesis of Primary Amines by Ruthenium-Catalyzed Amination of Secondary Alcohols with Ammonia. *Angew. Chemie Int. Ed.* **2010**, 49 (44), 8126–8129.
- (30) Del Zotto, A.; Baratta, W.; Sandri, M.; Verardo, G.; Rigo, P. Cyclopentadienyl Ru(II) Complexes as Highly Efficient Catalysts for the N-Methylation of Alkylamines by Methanol. Eur. J. Inorg. Chem. 2004, 2004, 524–529.
- (31) Singh Sisodia, O.; Sahay, A. N.; Pandey, D. S.; Agarwala, U. C.; Jha, N. K.; Sharma, P.; Toscano, A.; Cabrera, A. Synthesis and Characterization of Some Arene Hydrido-Complexes [Ru(H6-Arene)(EPh3)2H]+ (H6-Arene=benzene, p-Cymene or Hexamethylbenzene; E=P, As or Sb). Crystal Structure of [Ru(H6-C6H6)(PPh3)2H] BF4. J. Organomet. Chem. 1998, 560 (1–2), 35–40.
- (32) Churchill, M. R.; Hollander, F. J.; Hutchinson, J. P. An Accurate Redetermination of the Structure of Triruthenium Dodecacarbonyl, Ru3(CO)12. Inorg. Chem. 1977, 16 (10), 2655–2659.
- (33) Solari, E.; Gauthier, S.; Scopelliti, R.; Severin, K. Multifaceted Chemistry of [(Cymene)RuCl2]2 and PCy3. Organometallics 2009, 28 (15), 4519–4526.
- (34) Hall, E. O.; Crangle, J. An X-Ray Investigation of the Reported High-Temperature Allotropy of Ruthenium. Acta Crystallogr. 1957, 10 (3), 240–241.
- (35) Liu, S.-H.; Han, Z.-J.; Meng, T.; Luo, X.; Yuan, J.; Wu, Q.-G.; Chen, J.; Yu, G.-A. Novel Dinuclear and Trinuclear Ruthenium Clusters Derived from 2-Aryl-Substituted Indenylphosphines via C—H Bond Cleavage. Appl. Organomet. Chem. 2016, 31 (8), e3670.
- (36) Cifuentes, M. P.; Humphrey, M. G.; Skelton, B. W.; White, A. H. High-Nuclearity Ruthenium Carbonyl Cluster Chemistry. 2. Reaction of [Ru2(μ-H)(μ-NC5H4)2(CO)4(NC5H5)2][Ru10(μ-H)(M6-C) (CO)24] with Triphenylphosphine: Stepwise Apical Substitution on a "Giant Tetrahedral" Cluster. Organometallics 1995, 14 (3), 1536–1538.
- (37) Ellis, D.; Farrugia, L. J. X-Ray Crystal Structures of Ru3(μ-H)(μ-C,N-C5H4N)(CO)10-n(PiPr3)n, N=0,1: A A Case of the Hydride Following the Phosphine? *J. Clust. Sci.* 2005, 7 (1), 71–83.
- (38) Balaraman, E.; Khaskin, E.; Leitus, G.; Milstein, D. Catalytic Transformation of Alcohols to Carboxylic Acid Salts and H2 Using Water as the Oxygen Atom Source. Nat. Chem. 2013, 5 (2), 122–125.
- (39) Choi, J. H.; Heim, L. E.; Ahrens, M.; Prechtl, M. H. G. Selective Conversion of Alcohols in Water to Carboxylic Acids by in Situ Generated Ruthenium Trans Dihydrido Carbonyl PNP Complexes. *Dalt. Trans.* 2014, 43 (46), 17248–17254.
- (40) Malineni, J.; Keul, H.; Möller, M. A Green and Sustainable Phosphine-Free NHC-Ruthenium Catalyst for Selective Oxidation of Alcohols to Carboxylic Acids in Water. *Dalt. Trans.* 2015, 44 (39), 17409–17414.
- (41) Li, Y.; Nielsen, M.; Li, B.; Dixneuf, P. H.; Junge, H.; Beller, M. Ruthenium-Catalyzed Hydrogen Generation from Glycerol and Selective Synthesis of Lactic Acid. Green Chem. 2015, 17 (1), 193–198.
- (42) Raffa, G.; Dumeignil, F.; Paul, S.; Capet, F.; Nguyen, D. H.; Desset, S.; Gauvin, R. M.; Zhang, L.; Trivelli, X. Catalytic Conversion of Alcohols into Carboxylic Acid Salts in Water: Scope, Recycling, and Mechanistic Insights. ChemSusChem 2016, 9 (12), 1413–1423.
- (43) Santilli, C.; Makarov, I. S.; Fristrup, P.; Madsen, R. Dehydrogenative Synthesis of Carboxylic Acids from Primary Alcohols and Hydroxide Catalyzed by a Ruthenium N-Heterocyclic Carbene Complex. J. Org. Chem. 2016, 81 (20), 9931–9938.
- (44) Sarbajna, A.; Dutta, I.; Daw, P.; Dinda, S.; Rahaman, S. M. W.; Sarkar, A.; Bera, J. K. Catalytic Conversion of Alcohols to Carboxylic Acid Salts and Hydrogen with Alkaline Water. ACS Catal. 2017, 7 (4), 2786–2790.
- (45) Dai, Z.; Luo, Q.; Meng, X.; Li, R.; Zhang, J.; Peng, T. Ru(II) Complexes Bearing 2,6-Bis(Benzimidazole-2-Yl)Pyridine Ligands: A New Class of Catalysts for Efficient Dehydrogenation of Primary Alcohols to Carboxylic Acids and H2 in the Alcohol/CsOH System. J. Organomet. Chem. 2017, 830, 11–18.
- (46) Singh, A.; Singh, S. K.; Saini, A. K.; Mobin, S. M.; Mathur, P. Facile Oxidation of Alcohols to Carboxylic Acids in Basic Water Medium by Employing Ruthenium Picolinate Cluster as an Efficient Catalyst. Appl. Organomet. Chem. 2018, 32 (12), 1–10.
- (47) Chatt, J.; Shaw, B. L.; Field, A. E. The Formation of Hydrido- and Carbonyl Complexes of Ruthenium by Reaction of Certain of Its Complexes with Alcohols. J. Chem. Soc. 1964, 3466–3475.
- (48) Vaska, L.; DiLuzio, J. W. Complex Carbonyl Hydrides of Osmium and Ruthenium. *J. Am. Chem. Soc.* **1961**, 83 (5), 1262–1263.

- (49) Capitani, D.; Mura, P. Do Paramagnetic Platinum Metal Hydrides Really Exist? A Reinvestigation of the Synthesis and Magnetochemical Properties of Ir(H)x(Cl)2(P-i-Pr3)2 (1). *Inorganica Chim. Acta* 1997, 258, 169–181.
- (50) Harris, P.; Madsen, R.; Olsen, E. P. K.; Singh, T.; Andersson, P. G. Experimental and Theoretical Mechanistic Investigation of the Iridium-Catalyzed Dehydrogenative Decarbonylation of Primary Alcohols. J. Am. Chem. Soc. 2014, 137 (2), 834–842.
- (51) Nikolaou, S.; Toma, H. E. Synthesis, Spectroscopy and Electrochemistry of a μ-Oxo-Triruthenium Cluster Containing a Bridged Bis(2,2'-Bipyridyl)Ruthenium(II) Moiety. Polyhedron 2001, 20 (3–4), 253–259
- (52) Dai, F. R.; Wu, Y. H.; Zhang, L. Y.; Li, B.; Shi, L. X.; Chen, Z. N. Spectroscopic, Electrochemical, and DFT Studies of Oxo-Centered Triruthenium Cluster Complexes with a Bis(Tridentate) Triazine Ligand. Eur. J. Inorg. Chem. 2011, 1 (14), 2306–2316.

- (53) Cabeza, J. A.; Del Río, I.; Pérez-Carreño, E.; Pruneda, V. Reactivity of Cationic Triruthenium Carbonyl Clusters: From Pyrimidinium Ligands to N-Heterocyclic Carbenes. Organometallics 2011, 30 (5), 1148–1156.
- (54) Zhang, H. X.; Sasaki, Y.; Abe, M.; Zhang, Y.; Ye, S.; Osawa, M. Preparation, Spectroscopy, and Electrochemistry of Cyano-Bridged Bis(Oxo-Centered-Hexa(μ-Acetato)-Triruthenium) Complexes. J. Organomet. Chem. 2015, 797, 29–36.
- (55) Connelly, N. G.; Geiger, W. E. Chemical Redox Agents for Organometallic Chemistry. Chem. Rev. 1996, 96, 877–910.
- (56) Evans, D. F. The Determination of the Paramagnetic Susceptibility of Substances in Solution by Nuclear Magnetic Resonance. J. Chem. Soc. 1959, 2003–2005.
- (57) Deutsch, J. L.; Poling, S. M. The Determination of Paramagnetic Susceptibility by NMR: A Physical Chemistry Experiment. J. Chem. Educ. 1969, 46 (3), 167–168.



TOC/Abstract Graphic. For Table of Contents Only